ipso-Substitution Reaction in the Convergent Stepwise Synthesis of Calix[8]arene with Regioselectively Functionalized Upper Rim

by **Hirohito Tsue***, **Kazutaka Enyo**, and **Ken-ichi Hirao**

Division of Material Science, Graduate School of Environmental Earth Science, Hokkaido University, Sapporo 060-0810, Japan

The acid-catalyzed multi-step synthesis of calix[8]arene **1**, which contains a regioselectively functionalized upper rim, has been investigated through the careful separation of the resulting by-products. A total of 11 types of cyclic and acyclic by-products were isolated and identified by spectral and microanalytical data. Semiempirical molecular-orbital calculations demonstrated that the synthetic process involves two types of reaction mechanism, one of which leads to the favorably constructed framework, while the other results in undesirable fragmentation reactions *via ipso*-substitution. A comparison of the theoretical predictions and the observed by-products revealed that steric hindrance, as well as the regioselectivity of the reaction, is also an important factor for determining the reaction pathway. A possible rationale is presented to explain the overall formation process leading to calix[8]arene **1** along with the by-products.

1. Introduction. – 'Calixarene' is a general term given to a series of macrocyclic phenol condensates, connected by methylene bridges, and play an important role in host-guest chemistry together with crown ethers and cyclodextrins [1–4]. Synthetic strategies for the construction of calixarene frameworks are generally classified into two main groups, *i.e.*, one-step and multi-step syntheses [1–3]. Although both strategies pose advantages and disadvantages for practical use, the choice depends mainly on the molecular structure of the desired system. The one-step strategy has been extensively utilized for preparing calixarenes with uniformly functionalized upper rims, and systematic and extensive studies by *Gutsche* and co-workers [5] enable the ring size to be controlled by simply adjusting the reaction conditions used. On the other hand, the multi-step synthesis has mainly been applied to the synthesis of calixarenes containing different substituents at the upper rim [1][6]. Whereas the latter methodology has permitted the synthesis of regioselectively substituted calixarenes with well-defined molecular structures, this method is usually associated with long and tedious reaction steps that cause poor overall yields and also present a large barrier to its conventional use. Nonetheless, because of the synthetic flexibility and simplicity, we have previously employed the latter strategy for preparing the first calix[8]arene **1** [7], in which the upper rim is regioselectively modified by two different types of substituents. However, contrary to prior expectation, a variety of linear and cyclic by-products, including a ring-shrunken calix[6]arene, were found to be formed as contaminants in the synthesis of **1**. This foregoing finding strongly prompted us to isolate and identify these by-products and to investigate the reaction mechanism by which they are produced. In this paper, we report a full account of the molecular structures of the by-products, and of the key reaction mechanism *via ipso*-substitution, which appears to be commonly involved in the multi-step synthesis of calixarenes.

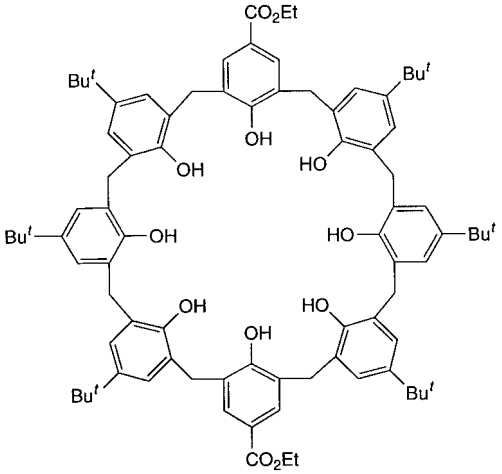

1

2. Results and Discussion. – 2.1. *Synthesis.* According to the previous report [7], calix[8]arene **1** was prepared by the application of a convergent '7 + 1' fragment condensation, which is an extension of *Böhmer*'s '3 + 1' methodology [3][6]. The '7' fragment **4** was prepared in 20% yield by acid-catalyzed condensation of 4-(*tert*-butyl)phenol condensate **2** [8] and bis(hydroxymethyl)benzoate **3** [9]. Subsequent acid-promoted ring closure of equimolar amounts of the '7' fragment **4** and the '1' fragment **3** afforded the desired calix[8]arene **1** in 8.5%.

2.2. *By-products.* The fairly low yields in the syntheses of **4** and **1** are reflected in the fact that both reaction steps were accompanied by the formation of a variety of by-products, which were carefully purified by repetitive flash column chromatography (FC) and identified by their spectral and microanalytical data. *Figs. 1* and *2* schematically summarize the molecular structures of the by-products isolated from the two reaction steps.

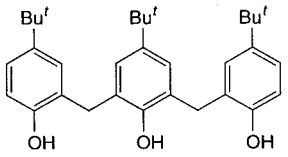

2

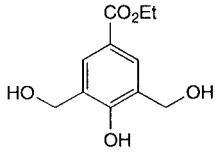

3

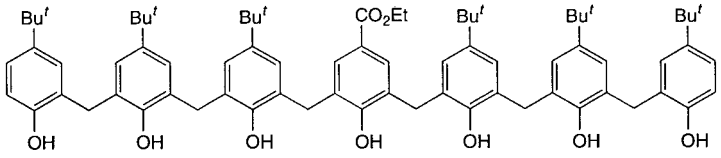

4

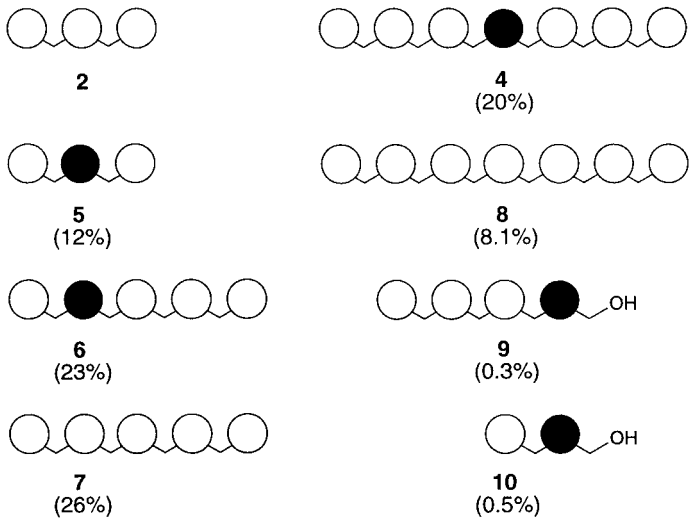

Fig. 1. *Schematic representation of the by-products with acyclic molecular structures and their yields in the first step* **2** + **3** → **4**. Filled (black) circle = 5-(ethoxycarbonyl)-2-hydroxy-1,3-phenylene; empty circle = 5-(*tert*-butyl)-2-hydroxy-1,3-phenylene.

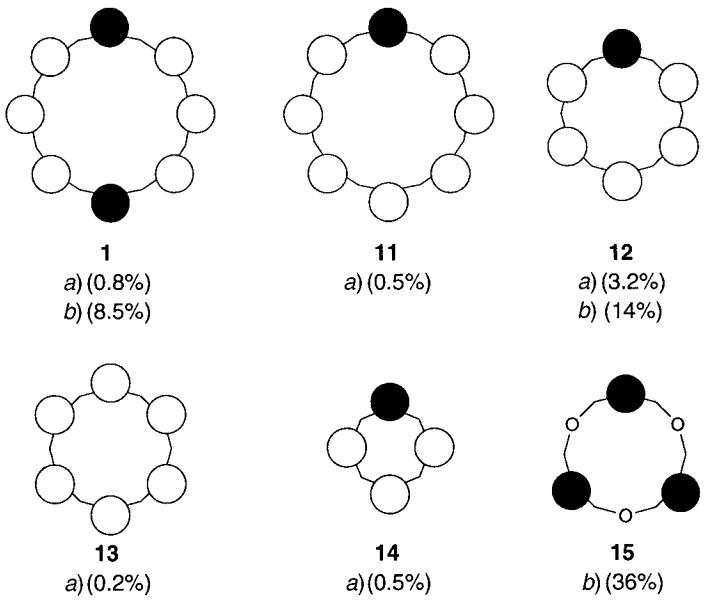

Fig. 2. *Schematic representation of the by-products with cyclic molecular structures and their yields* a) *in the first step* **2** + **3** → **4** *and* b) *in the second step* **4** + **3** → **1**. Filled (black) circle = 5-(ethoxycarbonyl)-2-hydroxy-1,3-phenylene; empty circle = 5-(*tert*-butyl)-2-hydroxy-1,3-phenylene.

In the first step **2** + **3** → **4**, a total of 82% of the reaction products was recovered and identified, and all the compounds which are depicted in *Figs. 1* and *2* were obtained, with the sole exception of homooxacalix[3]arene **15**. Acyclic products were trimer **5**, two types of pentamers **6** and **7**, two types of heptamers **4** and **8**, and two types of terminally hydroxymethylated condensates **9** and **10**, along with the unreacted **2**, while the cyclic molecules were two types of calix[8]arenes **1** and **11**, two types of calix[6]arene derivatives **12** and **13**, and calix[4]arene **14**. On the other hand, in the second step **4** + **3** → **1**, a total of 54% of the product mixture was identified, and only cyclic by-products, such as ring-shrunken calix[6]arene **12** and homooxacalix[3]arene **15** were obtained, along with the recovered heptamer **4** and the desired calix[8]arene **1**. An important point in these two reactions is that the starting materials **2**–**4** would not be expected to afford compounds such as **5**–**8** and **10**–**13**, although the formations of homooxacalix[3]arene **15** from **3** and of calix[4]arene **14** from **2** and **3** are easily understandable.

2.3. *Acid Lability.* To elucidate the reaction mechanism affording a variety of by-products, the acid lability of **1**, **2**, and **4** were examined by exposing each compound to acidic conditions, which were essentially identical to those used for the acid-catalyzed condensation reactions **2** + **3** → **4** and **4** + **3** → **1**. However, these compounds were recovered quantitatively and revealed no detectable changes, indicating that they are stable under these conditions. It is thus reasonable to assume that none of the by-products are generated directly from molecules **1**, **2**, and **4**. It is particularly interesting to note that calixarenes **12**–**14** are not formed by the direct [8]-to-[6] or [8]-to-[4] shifts of **1**, at least under the reaction conditions examined herein, although *Mendoza et al.* [10] reported the direct transformation of a calix[6]arene into a calix[4]arene under acidic conditions, and *Gutsche* and co-workers also reported a similar molecular mitosis from 4-(*tert*-butyl)calix[8]arene to the bimolecular 4-(*tert*-butyl)calix[4]arene in the presence of NaOH [11].

In contrast to the stability of **1**, **2**, and **4**, the similar treatment of by-product **9** under the same acidic conditions resulted in the formation of a complicated mixture, as shown by TLC. Considering the synthetic processes of the target compound **1** and the intermediate **4**, the results of this experiment clearly suggest that the benzyl alcohol moiety present in **3**, **9**, and **10** serves as a trigger for inducing side reactions from which the by-products shown in *Figs. 1* and *2* are derived.

2.4. *Reaction Mechanism*. To further explore the reaction mechanism, an aromatic electrophilic substitution reaction between phenol condensate **2** and benzyl cation **16**, which could be generated *in situ* from benzyl alcohol **3** and the acid catalyst TsOH, was analyzed by means of a semiempirical molecular-orbital calculation based on MOPAC PM3 [12][13]. As shown in *Fig. 3*, the orbital coefficients of the HOMO (highest occupied molecular orbital) of **2** appeared only in one of the terminal phenol moieties. The LUMO (lowest unoccupied molecular orbital) of **16** is shown in *Fig. 4*.

According to *Klopman*'s general perturbation equation (*Eqn. 1*) [14], perturbation energies (ΔE) between the frontier molecular orbitals of the phenol condensate **2** and the benzyl cation **16** were estimated. In this equation, Q_A and Q_B are atomic charges of reactants A and B, R_{AB} is the distance separating them, ε is the dielectric constant of the reaction medium (2.27401 for benzene [15]), C_A and C_B are the orbital coefficients at one site of interaction, $\Delta\beta$ is the interorbital interaction integral, and E_A and E_B are the

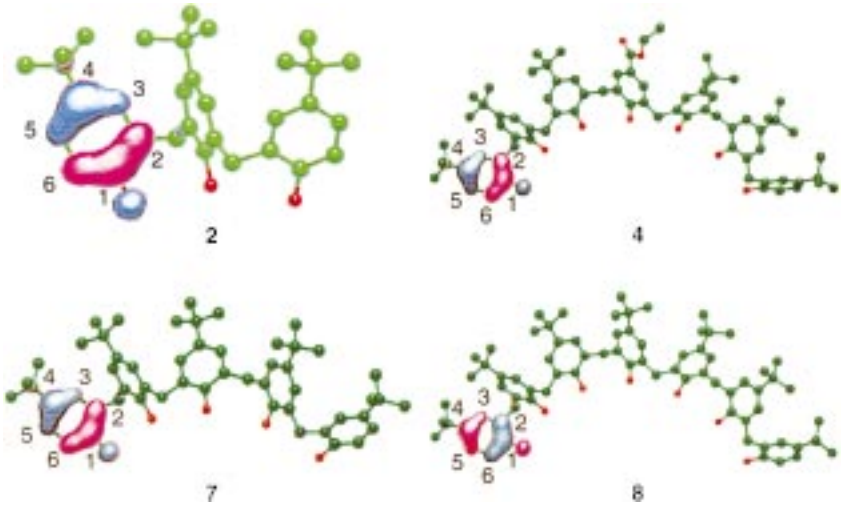

Fig. 3. *PM3-Calculated highest occupied molecular orbitals of phenol condensates* **2**, **4**, **7**, *and* **8**. H-Atoms are omitted for clarity. Arbitrary numbering of the terminal phenol moiety.

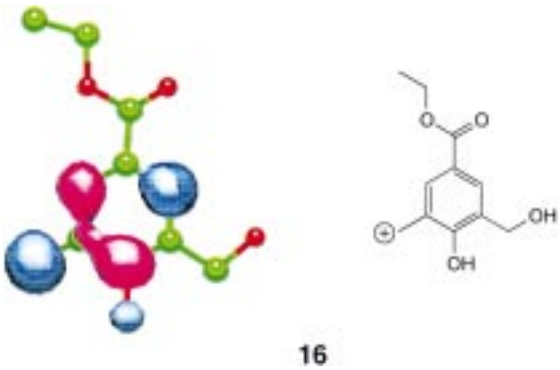

Fig. 4. *PM3-Calculated lowest unoccupied molecular orbital of benzyl cation* **16**. H-Atoms are omitted for clarity.

energy levels of the relevant molecular orbitals. Parameters R_{AB} and $\Delta\beta$ were set to be 2.5 Å and -2.63 eV [16], respectively, since preliminary PM3 calculations on the transition states in the aromatic electrophilic substitution reactions between **2** and **16** revealed that they were located *ca.* 2.5 Å apart from each other at around the saddle point.

$$\Delta E = -\frac{Q_A Q_B}{R_{AB}\varepsilon} + \frac{2(C_A C_B \Delta\beta)^2}{|\, E_A - E_B \,|} \tag{1}$$

As summarized in the *Table*, the theoretical calculations clearly showed that the *ortho*- and *para*-positions of the ring are susceptible to attack by the electrophile **16**. The regioselectivity was estimated to increase in the order C(6) < C(2) < C(4) (for

Scheme 1. *Competitive Reaction Pathways in the Aromatic Electrophilic Substitution Reaction of* **2** *and* **16**. Paths *a*) and *b*) represent electrophilic attack at positions C(6) and C(2), respectively.

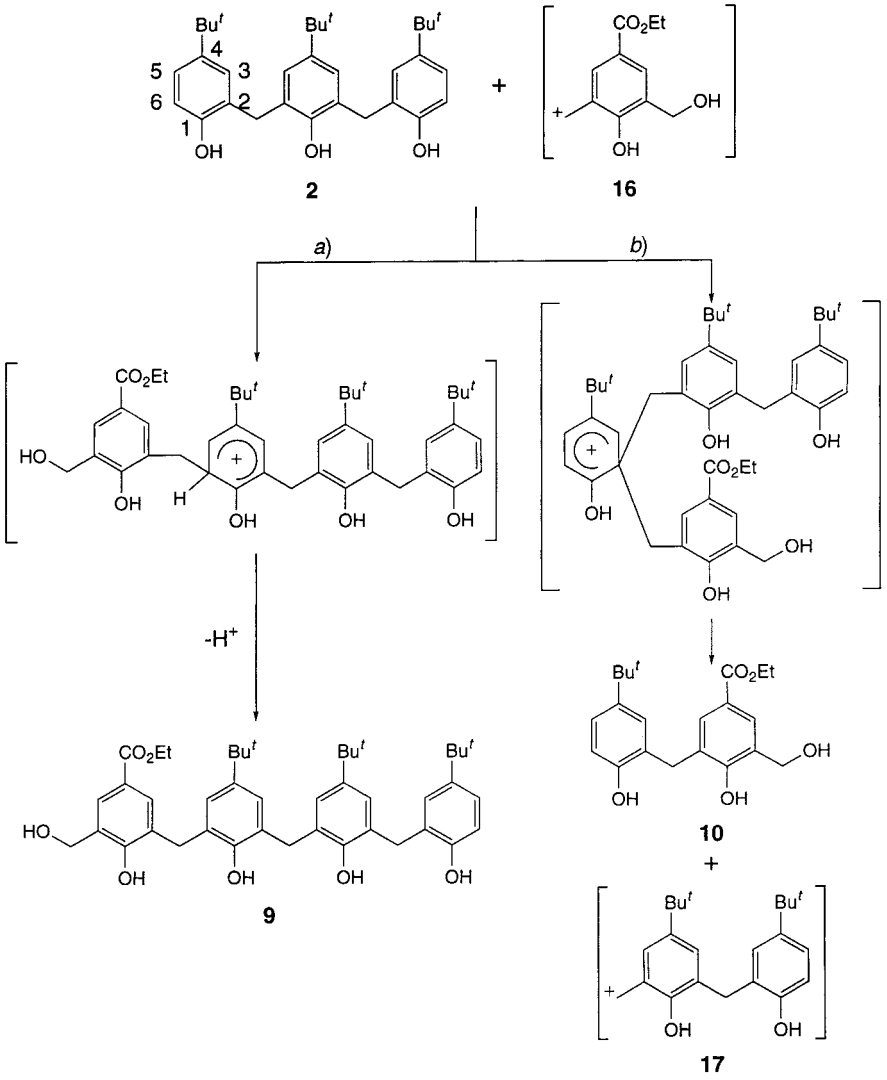

numbering, see *Fig. 3* and *Scheme 1*). In other words, the point of this theoretical prediction is that a reaction at position C(6) of **2** would favorably extend the linear structure of the product to give **9**, whereas that at position C(2) leads to an undesirable fragmentation reaction through a *Meisenheimer* complex to give a benzyl alcohol **10** and a benzyl cation **17**, as illustrated in *Scheme 1*.

This prediction is in reasonable agreement with the experimental result that compound **10** was isolated as a by-product from the reaction mixture. On the other hand, position C(4) of **2** was calculated to be the most reactive site, and the *tert*-butyl

cation would be expected to be a good leaving group. Nevertheless, the electrophilic attack at position C(4) does not occur, mainly due to the steric hindrance arising from the bulky *tert*-butyl group. Indeed, none of the corresponding by-products were detected among the reaction products. Consequently, the formation of the various by-products can be attributed to the participation of an additional reaction pathway, which would result from the newly formed benzyl alcohol **10** and benzyl cation **17**, which are capable of reacting with other molecules present in the same reaction system.

Table. *Calculated Perturbation Energies* (ΔE) *in the Aromatic Electrophilic Substitution Reactions of Benzyl Cation* **16** *with Phenol Condensates* **2**, **4**, **7**, *and* **8**. For numbering, see *Fig. 3* and *Scheme 1*.

	ΔE [eV]					
	C(1)	C(2)	C(3)	C(4)	C(5)	C(6)
2	0.63	0.48	0.16	0.84	0.21	0.36
4	0.65	0.51	0.16	0.87	0.22	0.36
7	0.65	0.51	0.16	0.87	0.22	0.36
8	0.66	0.51	0.16	0.87	0.22	0.36

Similarly, the other phenol condensates **4**, **7**, and **8** were predicted to have reactivities similar to **2**. As seen from *Fig. 3*, the orbital coefficients of the HOMOs of these molecules were also found only in one terminus, and the regioselectivities of the aromatic electrophilic substitution reaction with benzyl cation **16** were calculated to increase in the same order as that predicted for **2** (*Table*). Consequently, essentially the same reaction mechanism as that shown in *Scheme 1* would be applicable to the aromatic electrophilic substitution reactions of **4**, **7**, and **8**, which would be the key intermediates for the formation of calixarenes **11**–**13**.

Scheme 2 gives a reasonable explanation for the complete reaction pattern, which shows that the synthetic pathways leading to calix[8]arene **1** are associated with numerous competitive side reactions. The formation of **1**, **4**, **9**, **14**, and **15** can be easily understood, while it is likely that the other molecules are formed as above through undesirable fragmentation reactions *via ipso*-attack. Although the side reactions in *Scheme 2* remain to be established by actually examining the reactions of each by-product, it is possible to rationalize most of the formation processes by the theoretical and experimental results. In particular, from the mechanistic point of view, the present results are in good agreement with *Gutsche*'s recent study of the reaction mechanism, which involves *ipso*-substitution in the acid-induced one-step formation of calix[*n*]arenes ($n = 4-20$) from linear oligomers of 4-(*tert*-butyl)phenol and formaldehyde [17]. As a consequence, it seems reasonable to presume that the scheme represents a plausible, though inconclusive, interpretation for explaining the complete reaction pathways leading to calix[8]arene **1** and the observed by-products.

3. Conclusion. – The present study established that the formation of calix[8]arene **1** is very sensitive to regioselectivity of the aromatic electrophilic substitution reactions, although steric hindrance must also be taken into account as a factor determining the reaction pathway. Judging from our present result and those reported by *Böhmer et al.* [6a], who obtained a calix[4]arene as the exclusive product in the attempted synthesis

Scheme 2. *A Possible Explanation of All Reaction Pathways Starting from* **2** *and* **3**. The presence of a fragmentation reaction *via ipso*-substitution is designated as branched arrows.

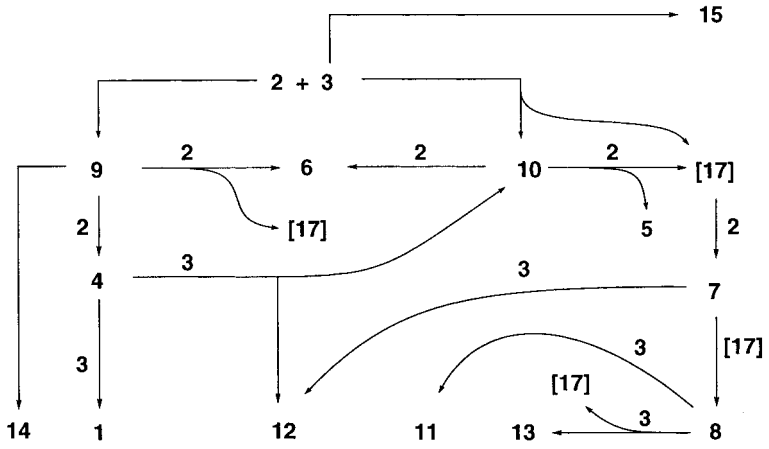

of a calix[5]arene by the '3 + 2' methodology, it seems quite likely that a fragmentation reaction *via ipso*-attack is frequently involved in the multi-step preparation of calixarenes, especially under acidic conditions, although a similar *ipso*-substitution in the heat-induced synthesis of calix[5]arenes under neutral conditions was also supposed to occur by *Biali et al.* [18]. Further investigation of the nature and generality of the undesirable pathways involving *ipso*-attack is currently under progress in our laboratory.

This work was financially supported, in part, by *Grant-in-Aid* for *Encouragement of Young Scientists* (Nos. 09740456 and 12740334) from the Ministry of Education, Science, Sports, and Culture, Japan. We are grateful to Ms. *Hiroko Matsumoto* and Ms. *Akiko Maeda* at the Center for Instrumental Analysis, Hokkaido University, for the measurement of elemental analysis. We are also indebted to the GC-MS and NMR Laboratory, Faculty of Agriculture, Hokkaido University, for FD-MS measurements.

Experimental Part

General. Organic solvents were purified by the standard procedure. Anh. benzene was prepared by distillation from CaH_2 under anh. conditions prior to use. Reagents were purchased at the highest commercially available grade and used without further purification, and compounds **2** and **3** were prepared according to the described procedure [8][9]. Flash column chromatography (FC): *Merck* silica gel *60* (particle size 0.040–0.063 mm). TLC: 0.25-mm *Merck* silica gel plates *60F-254*; detection by UV light. M.p.: *Yanagimoto MP-J3* and/or *-MP-500D* micro-melting-point apparatuses; uncorrected. FT-IR Spectra: *Jeol FT/IR-230* spectrometer. ^{1}H-NMR Spectra: *Jeol EX-400* spectrometer; chemical shifts δ in ppm rel. to Me_4Si as internal standard (= 0 ppm). MS: *Jeol JMS-AX500* and/or *JMS-SX102A* instruments. Elemental analyses: *Yanagimoto MT-5*. Semiempirical molecular-orbital calculations based on PM3 [13] were carried out with the MOPAC97 [12] program package implemented in WinMOPAC Version 2.0, *Fujitsu Limited*, Tokyo, Japan, 1998.

First Step **2** + **3** → **4**. A heterogeneous mixture of **2** (6.36 g, 13.4 mmol), **3** (1.0015 g, 4.4269 mmol), and TsOH (69.5 mg, 404 μmol) in anh. benzene (185 ml) was refluxed for 24 h; the suspension changed to a pale yellow soln. before reflux started. After cooling to r.t., the mixture was washed with sat. aq. $NaHCO_3$ soln. (2 × 300 ml) and brine (2 × 300 ml), dried (Na_2SO_4), and evaporated. The pale yellow solid (6.84 g) was purified by repetitive FC (silica gel). Purification by FC was repeated 19 times to separate the contents, solvent polarities ranging from $CHCl_3$/hexane 3 : 2 to $CHCl_3$/AcOEt 4 : 1. Unreacted **2** (2.3226 g) was recovered, and **4** (1.0093 g, 20.0%) was obtained along with **1** (23.0 mg, 0.78%), **5** (261.4 mg, 12.0%), **6** (818.1 g, 22.7%), **7** (901.8 mg,

25.5%), **8** (201.1 g, 8.1%), **9** (9.3 mg, 0.31%), **10** (8.4 mg, 0.53%), **11** (10.2 mg, 0.53%), **12** (69.8 mg, 3.2%), **13** (3.4 mg, 0.24%), and **14** (14.4 mg, 0.49%).

Second Step **3** + **4** → **1**. A suspension of **3** (198.2 mg, 876.1 μmol), **4** (1.0074 g, 884.0 μmol), and TsOH (6.3 mg, 37 μmol) in anh. benzene (90 ml) was heated under reflux for 24.5 h; the suspension became a yellow soln. prior to reflux. After cooling to r.t., the solvent was evaporated, the residue taken up in $CHCl_3$ (100 ml), the soln. washed with sat. aq. $NaHCO_3$ soln. (2 × 150 ml) and brine (150 ml), dried (Na_2SO_4), and evaporated, and the resulting pale yellow solid (1.23 g) subjected to repetitive FC (silica gel; 4 ×), with solvent polarities ranging from $CHCl_3$/hexane 7:3 to $CHCl_3$/AcOEt 19:1. Unreacted **4** (385.7 mg) was recovered, and **1** (99.5 mg, 8.5%) was obtained along with **12** (118.4 mg, 13.7%) and **15** (65.1 g, 35.7%).

*Diethyl 11,17,23,35,41,47-Hexa(*tert*-butyl)-49,50,51,52,53,54,55,56-octahydroxycalix[8]arene-5,29-dicarboxylate*[1]) (**1**): Colorless fine powder from $CHCl_3$/hexane. R_f 0.50 (silica gel, $CHCl_3$/hexane 7:3). M.p. >450° (dec.). IR (KBr): 3232, 1718. ^{1}H-NMR ($CDCl_3$, 400 MHz): 10.21 (br. *s*, 2 H); 9.37 (br. *s*, 2 H); 9.3 (br. *s*, 4 H); 7.87 (*s*, 4 H); 7.22 (*d*, *J* = 2.4, 4 H); 7.20 (*d*, *J* = 2.4, 4 H); 7.19 (*s*, 4 H); 4.33 (br. *s*, 12 H); 3.54 (br. *s*, 8 H); 1.36 (*t*, *J* = 7.1, 6 H); 1.26 (*s*, 36 H); 1.25 (*s*, 18 H). FD-MS: 1328 (M^+). Anal. calc. for $C_{86}H_{104}O_{12}$: C 77.68, H 7.88; found: C 77.51, H 7.93.

*4-(*tert*-Butyl)-2,6-bis{[5-(*tert*-butyl)-2-hydroxyphenyl]methyl}phenol* (**2**): Colorless solid from benzene. R_f (silica gel, $CHCl_3$/AcOEt 9:1) 0.53. M.p. 220–221° ([8]: 219–221°).

Ethyl 4-Hydroxy-3,5-bis(hydroxymethyl)benzoate (**3**): Colorless solid from $CHCl_3$. R_f (silica gel, $CHCl_3$/AcOEt 7:3) 0.12. M.p. 137–138° ([9]: 139°).

*Ethyl 3,5-Bis{[5-(*tert*-butyl)-3-{[5-(*tert*-butyl)-3-{[5-(*tert*-butyl)-2-hydroxyphenyl]methyl}-2-hydroxyphenyl]methyl}-2-hydroxyphenyl]methyl}-4-hydroxybenzoate* (**4**): Colorless solid from benzene/hexane. R_f (silica gel, $CHCl_3$) 0.38. M.p. 181.5–184.3° (dec.). IR (KBr): 3274, 1685. ^{1}H-NMR ($CDCl_3$, 400 MHz): 10.92 (br. *s*, 1 H); 9.98 (br. *s*, 2 H); 9.74 (br. *s*, 2 H); 9.41 (br. *s*, 2 H); 7.85 (*s*, 2 H); 7.31 (*d*, *J* = 2.2, 2 H); 7.24 (*d*, *J* = 2.4, 2 H); 7.23 (*d*, *J* = 2.2, 2 H); 7.20 (*d*, *J* = 2.4, 2 H); 7.18 (*d*, *J* = 2.2, 2 H); 7.02 (*dd*, *J* = 8.5, 2.2, 2 H); 6.75 (*d*, *J* = 8.5, 2 H); 4.32 (*q*, *J* = 7.1, 2 H); 4.00 (br. *s*, 4 H); 3.92 (br. *s*, 8 H); 1.35 (*t*, *J* = 7.1, 3 H); 1.29 (*s*, 18 H); 1.28 (*s*, 18 H); 1.25 (*s*, 18 H). FAB-MS: 1138 (M^+). Anal. calc. for $C_{75}H_{94}O_9$: C 79.05, H 8.31; found: C 78.96, H 8.30.

*Ethyl 3,5-Bis{[5-(*tert*-butyl)-2-hydroxyphenyl]methyl}-4-hydroxybenzoate* (**5**): Colorless solid from benzene/hexane. R_f 0.41 (silica gel, $CHCl_3$/AcOEt 9:1). M.p. 172–175° ([7]: 170°).

*Ethyl 3-{[5-(*tert*-Butyl)-2-hydroxyphenyl]methyl}-5-{[5-(*tert*-butyl)-3-{[5-(*tert*-butyl)-3-{[5-(*tert*-butyl)-2-hydroxyphenyl]methyl}-2-hydroxyphenyl]methyl}-2-hydroxyphenyl]methyl}-4-hydroxybenzoate* (**6**): Colorless solid from benzene/hexane. R_f (silica gel, $CHCl_3$/AcOEt 9:1) 0.62. M.p. 138–140°. IR (KBr): 3253, 1695. ^{1}H-NMR ($CDCl_3$, 400 MHz): 10.05 (br. *s*, 1 H); 9.22 (br. *s*, 1 H); 9.13 (br. *s*, 1 H); 8.73 (br. *s*, 1 H); 8.57 (br. *s*, 1 H); 7.89 (*d*, *J* = 2.2, 1 H); 7.85 (*d*, *J* = 2.2, 1 H); 7.32 (*m*, 2 H); 7.14 (*m*, 6 H); 6.89 (*d*, *J* = 8.3, 1 H); 6.79 (*d*, *J* = 8.6, 1 H); 4.34 (*q*, *J* = 7.1, 2 H); 3.90 (*s*, 2 H); 3.89 (*s*, 2 H); 3.85 (*s*, 2 H); 3.82 (*s*, 2 H); 1.37 (*t*, *J* = 7.1, 3 H); 1.28 (*s*, 9 H); 1.27 (*s*, 9 H); 1.26 (*s*, 9 H); 1.24 (*s*, 9 H). FD-MS: 814 (M^+). Anal. calc. for $C_{53}H_{66}O_7 \cdot 1.5\ H_2O$: C 75.59, H 8.26; found: C 75.76, H 8.39.

*4-(*tert*-Butyl)-2,6-bis{[5-(*tert*-butyl)-3-{[5-(*tert*-butyl)-2-hydroxyphenyl]methyl}-2-hydroxyphenyl]methyl}phenol* (**7**): Colorless solid from benzene/hexane. R_f (silica gel, $CHCl_3$/AcOEt 9:1) 0.71. M.p. 218–221° ([19]: 217–218°).

*4-(*tert*-Butyl)-2,6-bis{[5-(*tert*-butyl)-3-{[5-(*tert*-butyl)-3-{[5-(*tert*-butyl)-2-hydroxyphenyl]methyl}-2-hydroxyphenyl]methyl}-2-hydroxyphenyl]methyl}phenol* (**8**): Colorless solid from benzene/hexane. R_f (silica gel, $CHCl_3$/hexane 7:3) 0.32. M.p. 253–256° ([19]: 252–254°).

*Ethyl 3-{[5-(*tert*-Butyl)-3-{[5-(*tert*-butyl)-3-{[5-(*tert*-butyl)-2-hydroxyphenyl]methyl}-2-hydroxyphenyl]methyl}-2-hydroxyphenyl]methyl}-4-hydroxy-5-(hydroxymethyl)benzoate* (**9**): Colorless solid from $CHCl_3$/hexane. R_f (silica gel, $CHCl_3$/AcOEt 7:3) 0.50. M.p. 191–193°. IR (KBr): 3376, 1685. ^{1}H-NMR ($CDCl_3$, 400 MHz): 10.17 (br. *s*, 1 H); 9.19 (br. *s*, 1 H); 9.06 (br. *s*, 1 H); 8.82 (br. *s*, 1 H); 7.85 (*d*, *J* = 2.0, 1 H); 7.68 (*d*, *J* = 2.0, 1 H); 7.22 (*d*, *J* = 2.4, 1 H); 7.18 (*d*, *J* = 2.4, 1 H); 7.14 (*m*, 2 H); 7.09 (*d*, *J* = 2.4, 1 H); 7.01 (*dd*, *J* = 2.4, 8.5, 1 H); 6.48 (*d*, *J* = 8.5, 1 H); 5.04 (*d*, *J* = 5.1, 2 H); 5.00 (br. *s*, 1 H); 4.27 (*q*, *J* = 7.1, 2 H); 3.90 (*s*, 2 H); 3.84 (*s*, 2 H); 3.78 (*s*, 2 H); 1.31 (*t*, *J* = 7.1, 3 H); 1.26 (*s*, 9 H); 1.23 (*s*, 9 H); 1.22 (*s*, 9 H). FD-MS: 682 (M^+). Anal. calc. for $C_{43}H_{54}O_7 \cdot 0.5\ H_2O$: C 74.65, H 8.01; found: C 74.75, H 8.07.

*Ethyl 3-{[5-(*tert*-Butyl)-2-hydroxyphenyl]methyl}-4-hydroxy-5-(hydroxymethyl)benzoate* (**10**): Colorless solid from $CHCl_3$/hexane. R_f (silica gel, $CHCl_3$/AcOEt 7:3) 0.29. M.p. 114–117°. IR (KBr): 3367, 3248, 1693.

---

[1]) Calix[8]arene = nonacyclo[43.3.1.1^{3,7}.1^{9,13}.1^{15,19}.1^{21,25}.1^{27,31}.1^{33,37}.1^{39,43}]hexapentaconta-1(49),3,5,7(56),9,11,13-(55),15,17,19(54),21,23,25(53),27,29,31(52),33,35,37(51),39,41,43(50),45,47-tetracosaene.

^{1}H-NMR ($CDCl_3$, 400 MHz): 9.02 (br. *s*, 1 H); 7.96 (*d*, *J* = 2.1, 1 H); 7.63 (*d*, *J* = 2.1, 1 H); 7.29 (*d*, *J* = 2.5, 1 H); 7.13 (*dd*, *J* = 8.5, 2.5, 1 H); 6.78 (*d*, *J* = 8.5, 1 H); 6.68 (br. *s*, 1 H); 4.91 (*d*, *J* = 3.9, 2 H); 4.33 (*q*, *J* = 7.2, 2 H); 3.95 (*s*, 2 H); 2.52 (*t*, *J* = 3.9, 1 H); 1.36 (*t*, *J* = 7.2, 3 H); 1.28 (*s*, 9 H). FD-MS: 358 (M^+). Anal. calc. for $C_{21}H_{26}O_5 \cdot 0.05\ CHCl_3$: C 69.38, H 7.21, Cl 1.46; found: C 69.12, H 7.20, Cl 1.42.

*Ethyl 11,17,23,29,35,41,47-Hepta(*tert*-butyl)-49,50,51,52,53,54,55,56-octahydroxycalix[8]arene-5-carboxylate*[1]) (**11**): Colorless solid from $CHCl_3$/hexane. R_f (silica gel, $CHCl_3$/hexane 7:3) 0.74. M.p. >400° (dec.). IR (KBr) 3219, 1718. ^{1}H-NMR ($CDCl_3$, 400 MHz): 10.51 (br. *s*, 1 H); 10.22 (br. *s*, 1 H); 9.58 (br. *s*, 6 H); 7.87 (*s*, 2 H); 7.21 (*d*, *J* = 2.4, 2 H); 7.20 (*d*, *J* = 2.4, 2 H); 7.18 (*s*, 2 H); 7.17 (*s*, 8 H); 4.35 (br. *s*, 10 H); 3.55 (br. *s*, 8 H); 1.36 (*t*, *J* = 7.1, 3 H); 1.26 (*s*, 18 H); 1.25 (*s*, 45 H). FD-MS: 1312 (M^+). HR-FD-MS: 1312.798 (M^+, $C_{87}H_{108}O_{10}^+$; calc. 1312.795). Anal. calc. for $C_{87}H_{108}O_{10} \cdot H_2O$: C 78.59, H 8.40; found: C 78.46, H 8.32.

*Ethyl 11,17,23,29,35-Penta(*tert*-butyl)-37,38,39,40,41,42-hexahydroxycalix[6]arene-5-carboxylate*[2]) (**12**): Colorless powder from $CHCl_3$/hexane. R_f (silica gel, $CHCl_3$/hexane 7:3) 0.59. M.p. >400° (dec.). IR (KBr): 3137, 1714. ^{1}H-NMR ($CDCl_3$, 400 MHz): 11.07 (br. *s*, 1 H); 10.48 (br. *s*, 4 H); 10.25 (br. *s*, 1 H); 7.86 (*s*, 2 H); 7.17 (*d*, *J* = 2.0, 2 H); 7.16 (*s*, 6 H); 7.15 (*d*, *J* = 2.0, 2 H); 4.33 (*q*, *J* = 7.1, 2 H); 3.88 (br. *s*, 12 H); 1.37 (*t*, *J* = 7.1, 3 H); 1.27 (*s*, 9 H); 1.26 (*s*, 18 H); 1.25 (*s*, 18 H). FD-MS: 988 (M^+). Anal. calc. for $C_{65}H_{80}O_8 \cdot 1.1\ CHCl_3$: C 70.84, H 7.29, Cl 10.44; found: C 71.09, H 7.53, Cl 10.16.

*5,11,17,23,29,35-Hexa(*tert*-butyl)-37,38,39,40,41,42-hexahydroxycalix[6]arene*[2]) (**13**): Colorless solid from $CHCl_3$/hexane. R_f (silica gel, $CHCl_3$/hexane 7:3) 0.83. M.p. >300° [5b]: 372–374°).

*Ethyl 11,17,23-Tri(*tert*-butyl)-25,26,27,28-tetrahydroxycalix[4]arene-5-carboxylate* (= *Ethyl 11,17,23-Tri-(*tert*-butyl)-25,26,27,28-tetrahydroxypentacyclo[19.3.1.1^{3,7}.1^{9,13}.1^{15,19}]octacosa-1(25),3,5,7(28),9,11,13(27),15,17,19(26),21,23-dodecaene-5-carboxylate*; **14**): Colorless powder from $CHCl_3$/hexane. R_f (silica gel, $CHCl_3$/hexane 7:3) 0.30. M.p. >300°. IR (KBr): 3175, 1717. ^{1}H-NMR ($CDCl_3$, 400 MHz): 10.25 (br. *s*, 4 H); 7.76 (*s*, 2 H); 7.09 (*d*, *J* = 2.7, 2 H); 7.08 (*d*, *J* = 2.7, 2 H); 7.03 (*s*, 2 H); 4.29 (*q*, *J* = 7.1, 2 H); 4.25 (*m*, 4 H); 3.58 (br. *s*, 2 H); 3.49 (br. *s*, 2 H); 1.30 (*t*, *J* = 7.1, 3 H); 1.22 (*s*, 18 H); 1.19 (*s*, 9 H). FD-MS: 664 (M^+). Anal. calc. for $C_{43}H_{52}O_6 \cdot 0.4\ CHCl_3$: C 73.15, H 7.41, Cl 5.97; found: C 73.44, H 7.57, Cl 6.06.

Triethyl 25,26,27-Trihydroxy-2,3,10,11,18,19-hexahomo-3,11,19-trioxacalix[3]arene-7,15,23-tricarboxylate (= *Triethyl 25,26,27-Trihydroxy-3,11,19-trioxatetracyclo[19.3.1.1^{5,9}.1^{13,17}]heptacosa-1(25),5,7,9(27),13,15,17(26),21,23-nonaene-7,15,23-tricarboxylate*; **15**): Colorless fine powder from benzene/hexane. R_f (silica gel, $CHCl_3$/AcOEt 9:1) 0.63. M.p. 223–225°. IR (KBr): 3329, 1720. ^{1}H-NMR ($CDCl_3$, 400 MHz): 9.19 (*s*, 3 H); 7.86 (*s*, 6 H); 4.76 (*s*, 12 H); 4.33 (*q*, *J* = 7.1, 6 H); 1.37 (*t*, *J* = 7.1, 9 H). FD-MS: 624 (M^+). Anal. calc. for $C_{33}H_{36}O_{12}$: C 63.45, H 5.81; found: C 63.51, H 5.91.

REFERENCES

[1] C. D. Gutsche, 'Calixarenes Revisited', Ed. J. F. Stoddart, The Royal Society of Chemistry, Cambridge, 1998; 'Calixarenes: A Versatile Class of Macrocyclic Compounds', Eds. J. Vicens and V. Böhmer, Kluwer, Dordrecht, 1991; C. D. Gutsche, 'Calixarenes', Ed. J. F. Stoddart, The Royal Society of Chemistry, Cambridge, 1989.

[2] C. D. Gutsche, *Aldrichimica Acta* **1995**, *28*, 3; C. D. Gutsche, *Top. Curr. Chem*. **1984**, *123*, 1; C. D. Gutsche, *Acc. Chem. Res.* **1983**, *16*, 161.

[3] V. Böhmer, *Tetrahedron* **1995**, *34*, 713.

[4] P. Lhoták, S. Shinkai, *Yuki Gosei Kgaku Kyokaishi* **1995**, *53*, 963; M. Takeshita, S. Shinkai, *Bull. Chem. Soc. Jpn*. **1995**, *68*, 1088; S. Shinkai, *Tetrahedron* **1993**, *49*, 8933.

[5] a) C. D. Gutsche, M. Iqbal, *Org. Synth*. **1990**, *68*,234; b) C. D. Gutsche, B. Dhawan, M. Leonis, D. Stewart, *Org. Synth*. **1990**, *68*, 238; c) J. H. Munch, C. D. Gutsche, *Org. Synth*. **1990**, *68*, 243.

[6] See, *e.g.*, a) V. Böhmer, F. Marschollek, L. Zetta, *J. Org. Chem.* **1987**, *52*, 3200; b) L. Zetta, A. Wolff, W. Vogt, K.-L. Platt, V. Böhmer, *Tetrahedron* **1991**, *47*, 1911; c) K. No, J. E. Kim, K. M. Kwon, *Tetrahedron Lett*. **1995**, *36*, 8453.

[7] H. Tsue, M. Ohmori, K. Hirao, *J. Org. Chem*. **1998**, *63*, 4866; H. Tsue, K. Enyo, K. Hirao, *Org. Lett*. **2000**, *2*, 3071.

[8] B. Dhawan, C. D. Gutsche, *J. Org. Chem*. **1983**, *48*, 1536.

[9] A. Zinke, R. Ott, E. Leggewie, H. Hassanein, G. Zankl, *Monatsh. Chem.* **1956**, *87*, 552.

---

[2]) Calix[6]arene = heptacyclo[31.3.1.1^{3,7}.1^{9,13}.1^{15,19}.1^{21,25}.1^{27,31}]dotetraconta-1(37),3,5,7(42),9,11,13(41),15,17,19-(40),21,23,25(39),27,29,31(38),33,35-octadecaene.

[10] J. de Mendoza, P. M. Nieto, P. Prados, C. Sánchez, *Tetrahedron* **1990**, *46*, 671.
[11] C. D. Gutsche, M. Iqbal, D. Stewart, *J. Org. Chem*. **1986**, *51*, 742; B. Dhawan, S.-I. Chen, C. D. Gutsche, *Makromol. Chem*. **1987**, *188*, 921.
[12] J. J. P. Stewart, 'MOPAC97', Fujitsu Limited, Tokyo, Japan, 1998.
[13] J. J. P. Stewart, *J. Comput. Chem*. **1989**, *10*, 209.
[14] G. Klopman, in 'Chemical Reactivity and Reaction Paths', Ed. G. Klopman, Wiley & Sons, New York, 1974, p. 55.
[15] 'Organic Solvents: Physical Properties and Methods of Purification', 4th edn., Eds. J. A. Riddick, W. B. Bunger, and T. K. Sakano, Wiley & Sons, New York, 1986, p. 136.
[16] K. N. Houk, J. Sims, C. R. Watts, L. J. Luskus, *J. Am. Chem. Soc*. **1973**, *95*, 7301.
[17] D. R. Stewart, C. D. Gutsche, *J. Am. Chem. Soc*. **1999**, *121*, 4136.
[18] S. E. Biali, V. Böhmer, I. Columbus, G. Ferguson, C. Grüttner, F. Grynszpan, E. F. Paulus, I. Thondorf, *J. Chem. Soc., Perkin Trans. 2* **1998**, 2261.
[19] G. Casiraghi, M. Cornia, G. Ricci, G. Balduzzi, G. Casnari, G. D. Andreetti, *Makromol. Chem*. **1983**, *184*, 1363.

Received December 11, 2000